Hurricane Ida (2021)
Rapid Intensification Followed by Slow Inland Decay

Yi-Jie Zhu, Jennifer M. Collins, Philip J. Klotzbach, and Carl J. Schreck III

ABSTRACT: Hurricane Ida recently became one of the strongest hurricanes to hit Louisiana on record, with an estimated landfalling maximum sustained wind of 130 kt (1 kt ≈ 0.51 m s⁻¹). Although Hurricane Ida made landfall at a similar time of year and landfall location as Hurricane Katrina (2005), Ida's postlandfall decay rate was much weaker than Hurricane Katrina. This manuscript includes a comparative analysis of pre- and postlandfall synoptic conditions for Hurricane Ida and other historical major landfalling hurricanes (category 3+ on the Saffir–Simpson hurricane wind scale) along the Gulf Coast since 1983, with a particular focus on Hurricane Katrina. Abundant precipitation in southeastern Louisiana prior to Ida's landfall increased soil moisture. This increased soil moisture along with extremely weak overland steering flow likely slowed the storm's weakening rate postlandfall. Offshore environmental factors also played an important role, particularly anomalously high nearshore sea surface temperatures and weak vertical wind shear that fueled the rapid intensification of Ida just before landfall. Strong nearshore vertical wind shear weakened Hurricane Katrina before landfall, and moderate northward steering flow caused Katrina to move inland relatively quickly, aiding in its relatively fast weakening rate following landfall. The results of this study improve our understanding of critical factors influencing the evolution of the nearshore intensity of major landfalling hurricanes in the Gulf of Mexico. This study can help facilitate forecasting and preparation for inland hazards resulting from landfalling hurricanes with nearshore intensification and weak postlandfall decay.

KEYWORDS: Extreme events; Hurricanes/typhoons; Tropical cyclones

©2022 American Meteorological Society
For information regarding reuse of this content and general copyright information, consult the AMS Copyright Policy.

AFFILIATIONS: Zhu and Collins—School of Geosciences, University of South Florida, Tampa, Florida; **Klotzbach**—Department of Atmospheric Science, Colorado State University, Fort Collins, Colorado; **Schreck**—Cooperative Institute for Satellite Earth System Studies, North Carolina State University, Asheville, North Carolina

On 29 August 2021, Hurricane Ida made landfall in southern Louisiana as an extremely destructive storm with maximum sustained wind speeds of ~130 kt (1 kt ≈ 0.51 m s^{-1}; Beven et al. 2022) (Fig. 1a)—a category 4 hurricane on the Saffir–Simpson hurricane wind scale (SSHWS; Schott et al. 2012). On the same day 16 years earlier, Hurricane Katrina made devastating landfalls in southeast Louisiana and then in Mississippi, with its Louisiana landfall only ~130 km away from Ida's (Fig. 1b). Both storms are high on the list for strongest and costliest continental U.S. landfalling hurricanes, with consumer price index–adjusted damage in 2022 U.S. dollars from Katrina estimated at $180 billion and Ida estimated at $76.5 billion (Landsea and Franklin 2013; NOAA 2022). Though Ida and Katrina shared similar spatial and temporal characteristics, their nearshore intensity evolution and postlandfall decay were quite different. Hurricane Katrina rapidly intensified in the Gulf of Mexico and reached a peak intensity of 150 kt, only to weaken by 40 kt to 110 kt in the ~17 h prior to its initial landfall near Buras, Louisiana. After making a second landfall as a 105 kt hurricane just east of the Louisiana–Mississippi border, Katrina rapidly decayed to a tropical storm in ~9 h (Knabb et al. 2005). By comparison, the maximum sustained wind speed of Hurricane Ida continuously increased in the 48 h prior to landfall, with Ida making landfall at its peak intensity of 130 kt (Beven et al. 2022). Rather than rapidly decaying following
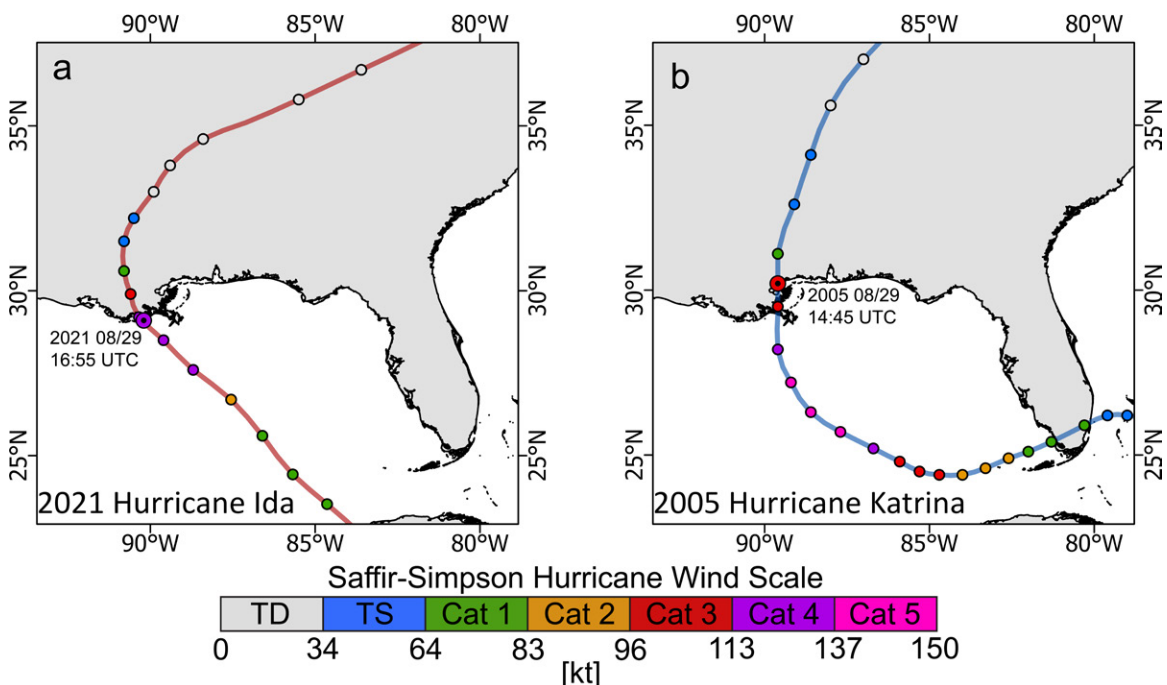

Fig. 1. Track of (a) Hurricane Ida (2021) and (b) Hurricane Katrina (2005). Each point represents the 6 h location of the storm with the intensity shown based on the Saffir–Simpson hurricane wind scale.

landfall, Ida's intensity only slowly decreased, with Ida retaining hurricane intensity even 12 h after landfall.

The distinct differences in the nearshore and postlandfall intensity changes between the two storms have underscored the need to better understand the nearshore intensity evolution of landfalling hurricanes, including 1) how Ida and Katrina's nearshore intensity evolution differs from other major (e.g., maximum sustained wind speed ≥ 96 kt; category 3+ on the SSHWS) hurricanes making landfall along the Gulf Coast and 2) what nearshore environmental factors were significantly different during Ida's landfall from other major hurricanes, especially Katrina.

In this manuscript, we first directly compare the synoptic conditions of Hurricane Ida and Katrina during their last 48 h over the ocean. The environmental factors examined in this study include sea surface temperature (SST) prior to landfall and land surface temperature after landfall as well as midtroposphere relative humidity, where higher values of these parameters are more favorable for hurricane intensification and maintenance (e.g., DeMaria and Kaplan 1994; Gray 1998; Emanuel 2007; Saunders et al. 2017; Wu et al. 2012). Vertical wind shear is another factor examined, with higher values of wind shear being unfavorable for nearshore intensification (e.g., Gray 1968; Kossin 2017). We also consider surface soil wetness, as recent studies show an important role for soil moisture in the postlandfall decay process (e.g., Kellner et al. 2012; Andersen and Shepherd 2017). In addition to the differences in Ida and Katrina's intensity changes pre- and postlandfall, we also note that these two systems had different translation speeds. Hurricane Katrina underwent postlandfall acceleration, while Hurricane Ida decelerated following landfall. As the movement of hurricanes along the Gulf Coast are primarily controlled by northward steering flow (Hassanzadeh et al. 2020), we also examine the meridional wind. The above environmental factors are then examined for other major historical landfalling hurricanes along the Gulf Coast.

Methods

Best track data and landfall criteria. The hurricanes' temporal and spatial information is taken from the National Hurricane Center's North Atlantic hurricane database (HURDAT2; Landsea and Franklin 2013) as archived in the International Best Track Archive for Climate Stewardship (IBTrACS; www.ncdc.noaa.gov/ibtracs/) version 4 (Knapp et al. 2010). The HURDAT2 dataset reports the maximum 1-min-averaged sustained wind speed (MSW) at 10 m for each 6 h interval. Only major hurricanes that made landfall along the Gulf Coast (excluding the west coast of the Florida peninsula) are used in this study. Landfall data are from the Atlantic Oceanographic and Meteorological Laboratory (AOML; www.aoml.noaa.gov/hrd/hurdat/UShurrs_detailed.html). Although hurricane data for the North Atlantic basin are generally considered reliable from the early 1970s after geostationary satellites were deployed (Landsea 2007), the Atlantic Hurricane Database Reanalysis Project (Delgado et al. 2018) currently ends in 1970. Hurricane landfalls are explicitly identified in the reanalyzed portion of HURDAT2 (e.g., 1851–1970) as well as from 1983 to onward. Given the increased uncertainty in landfall intensities from 1971 to 1982, we investigate Gulf Coast landfalling major hurricanes from 1983 to 2021 for data consistency purposes (Table 1). We take Katrina's final landfall (e.g., just east of the Louisiana–Mississippi border) as its landfall point (1445 UTC 29 August 2005).

Reanalysis data. The European Centre for Medium-Range Weather Forecasts (ECMWF) fifth-generation reanalysis dataset (ERA5) is employed for evaluating synoptic conditions (Hersbach et al. 2020). Sea surface temperature, land surface temperature (i.e., skin temperature), and volumetric soil water (0–7 cm depth) are retrieved from ERA5 on single levels, while 200, 500, and 850 hPa meridional and zonal winds as well as 500 hPa relative humidity

(RH) are taken from ERA5 on pressure levels. A dimensionless land–sea mask (values > 0.5) from ERA5 on single levels is applied to separate the ocean from the land surface. Both datasets are archived at hourly temporal resolution and at 0.25° × 0.25° spatial resolution, except for SST that is only updated once daily. For this study, we used a 3 h temporal resolution to calculate the mean of the parameters. The zonal and meridional winds are used to form the wind vector. Vertical wind shear (VWS) is calculated as the absolute difference of the wind vector between 200 and 850 hPa. The deep-layer meridional steering wind flow is defined as the weighted average of lower-level 850 hPa (25%), midlevel 500 hPa (50%), and higher-level 200 hPa (25%) winds. The calculations for the steering flow and VWS are made with the TC vortex removed following the approach used in Galarneau and Davis (2013). The reanalysis data are further masked within a 500 km radius (based on an equidistant conic projection) from each hurricane's landfall location to represent nearshore conditions (Fig. 2). The 500 km radius is based on the average of all Gulf Coast major landfalling hurricanes' translation speed during the 24 h prior to landfall (i.e., 21 km h^{-1} × 24 h ~ 500 km). Since previous studies also noted that ocean-to-atmosphere energy exchange often occurs near the eyewall (Cione and Uhlhorn 2003), and abundant soil moisture ("brown ocean" effect) can also act as a fuel supply for the intensification of landfalling storms (Andersen and Shepherd 2017; Nair et al. 2019), a smaller radius of 200 km is also employed to reflect the surface conditions from SST, land surface temperature, and soil moisture.

Table 1. List of Gulf Coast major landfalling hurricanes investigated in this study, along with their landfall intensity and the state where they made landfall. We use Katrina's landfall in Mississippi (e.g., 105 kt).

Year	Name	Landfalling wind (kt)	Landfalling state
1983	Alicia	100	Texas
1985	Elena	100	Mississippi
1992	Andrew	100	Louisiana
1995	Opal	100	Florida
1999	Bret	100	Texas
2004	Ivan	105	Alabama
2005	Dennis	105	Florida
2005	Katrina	105	Mississippi
2005	Rita	100	Louisiana
2017	Harvey	115	Texas
2018	Michael	140	Florida
2020	Laura	130	Louisiana
2020	Zeta	100	Louisiana
2021	Ida	130	Louisiana

Statistical significance test. We employ a two-tailed Student's *t* test to check for statistical significance throughout the manuscript. We evaluate statistical significance at the 5% level.

A general view of prelandfall environmental conditions for Ida and Katrina

We begin by examining the key factors that drove the differential pre- and postlandfall intensity changes between Ida and Katrina. In both cases, SSTs in the Gulf of Mexico were favorable for hurricane intensification. Gulf of Mexico SSTs in late August are
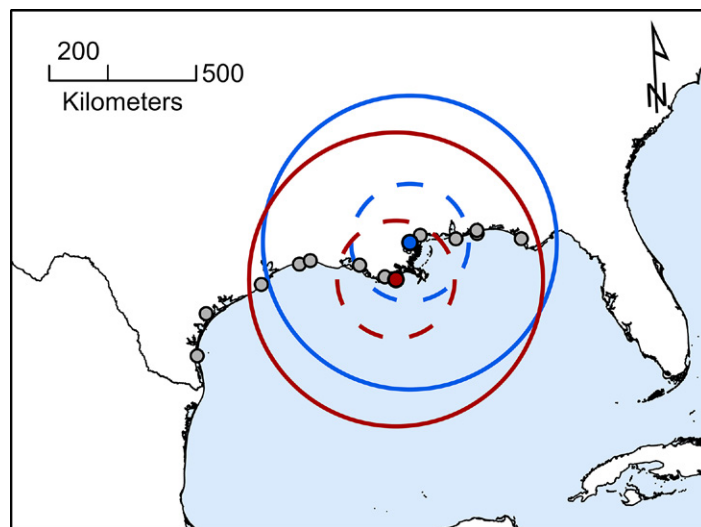

Fig. 2. Schematic of the nearshore spatial coverage with all major landfalling hurricane locations in this study shown with dots. The landfall location and 500 km nearshore spatial coverages of Hurricane Ida and Hurricane Katrina are depicted by red and blue dots and solid circles, respectively. The dashed circles denote a 200 km radius.
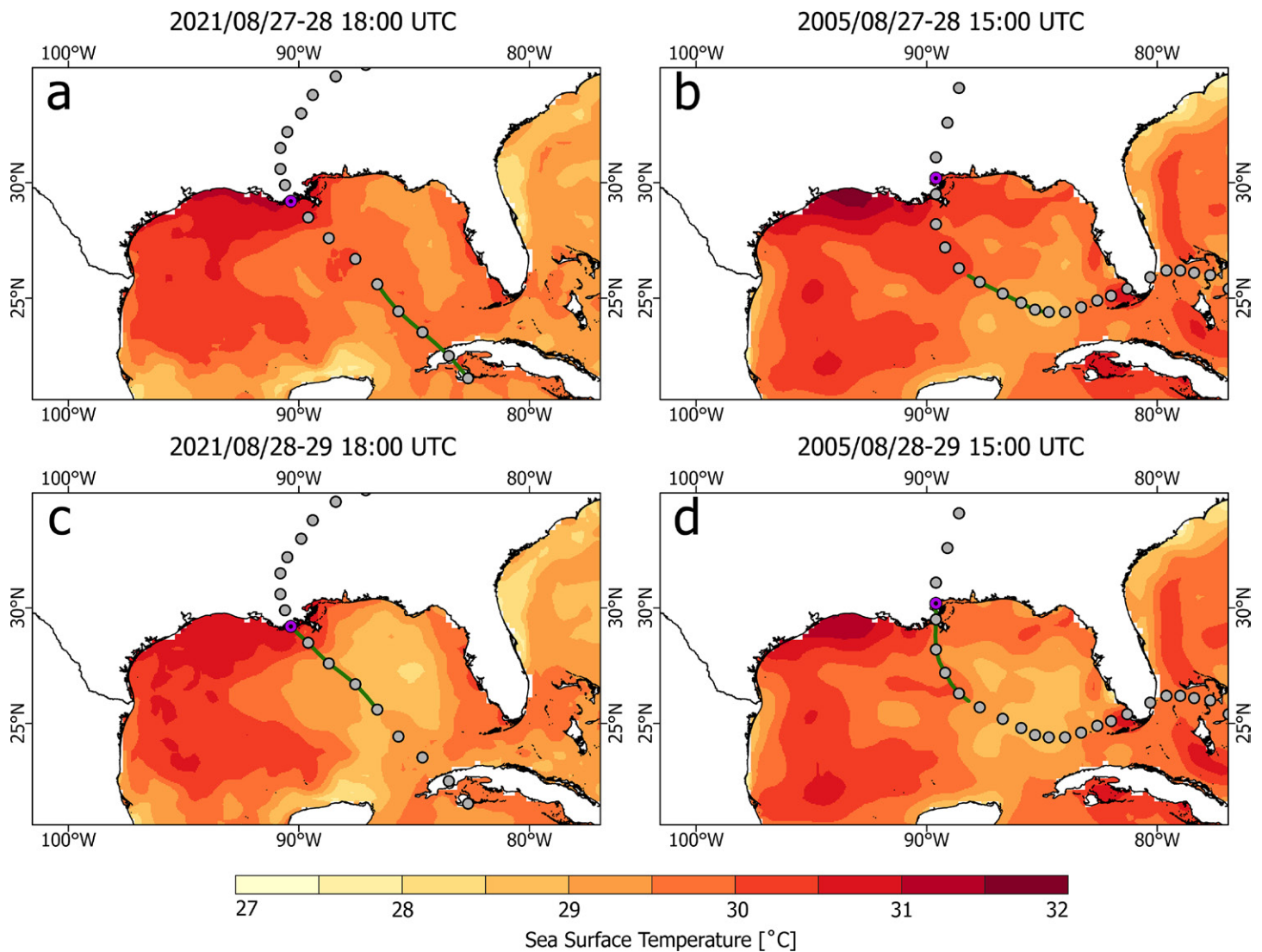
Fig. 3. Sea surface temperatures averaged during the prelandfall period of Hurricane Ida and Hurricane Katrina. For better visualization purposes, the 0.25° × 0.25° resolution from the source data are bilinearly resampled to 0.05° × 0.05°. The 6-hourly locations of the storm are marked in gray, with the landfall location highlighted in purple. The tracks over the 24 h averaging period are depicted with lines. (a) 48–24 h prior to Ida's landfall; (b) as in (a), but for Katrina; (c) 24–0 h before Ida's landfall; (d) as in (c), but for Katrina.

well above the SST threshold of ~26.5°C identified by previous studies for hurricane formation (e.g., Gray 1968; McTaggart-Cowan et al. 2015). Sea surface temperatures averaging ~29.5°C during the 24–48 h prelandfall period of Ida were favorable for intensification of the storm (Fig. 3a). Similarly favorable SST conditions were observed in the 24–48 h prelandfall period for Katrina, where a warm eddy supported further intensification of Katrina to its maximum intensity of 150 kt (Fig. 3b). In the 24 h prior to landfall, Ida continued to intensity over extremely warm SSTs, especially immediately prior to landfall (~30°C) (Fig. 3c), while Katrina weakened from its peak intensity over slightly cooler SSTs (~29°C) (Fig. 3d). These results are supported by a recent study showing the significance of nearshore shallow water heating for the intensification of landfalling tropical cyclones (TCs; Lok et al. 2021). While nearshore SSTs were slightly cooler for Katrina than they were for Ida, SSTs alone cannot explain the different nearshore intensity change patterns of Ida and Katrina. Sea surface temperatures were still sufficiently warm to support intensification with Katrina in the 24 h prior to landfall.

The midtropospheric moisture content was also more favorable for Ida than it was for Katrina. In the 24–48 h period prior to Ida's landfall, abundant moisture content was available ahead of Ida, especially over southern Louisiana (Fig. 4a). The average RH within a 200 km
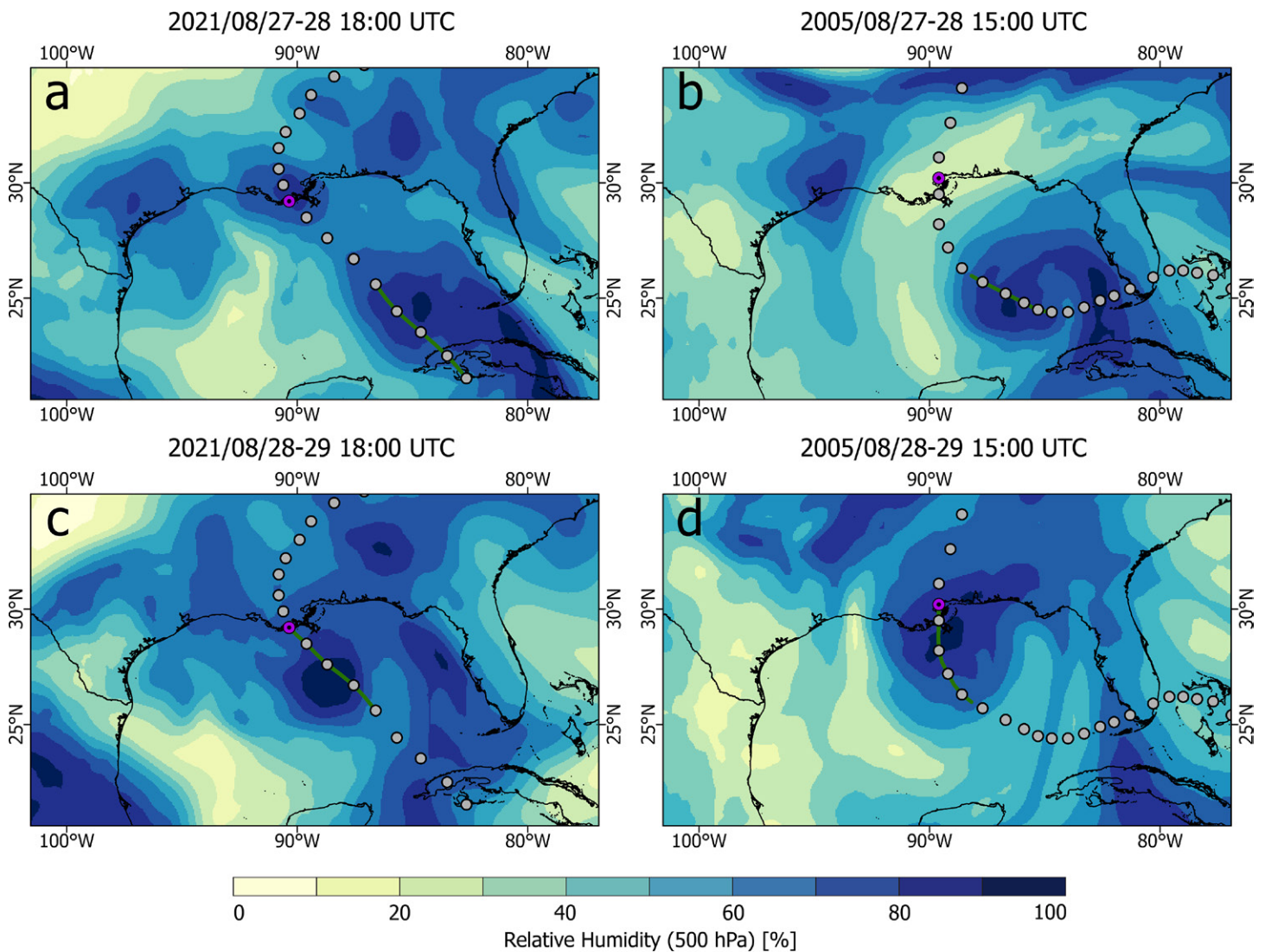
Fig. 4. As in Fig. 3, but for 500 hPa relative humidity.

radius of the landfall location during that period was 72%. The concentration of nearly saturated RH over southern Louisiana (~81% RH within a 50 km radius of the landfall location) implied the occurrence of precipitation. By comparison, drier air was apparent near the coast of Louisiana in the 24–48 h period prior to Katrina's landfall (Fig. 4b), where the average RH within a 200 km radius of the landfall location was ~30%. This dry air entrained into the western semicircle of Katrina and may have been one of the reasons that Katrina weakened in the 24 h prior to landfall (Knabb et al. 2005). When these two storms approached the coastline, they both advected substantial moisture inland (Figs. 4c,d), as would be expected given the large amount of storm moisture that is carried when passing over a warm ocean (Li and Chakraborty 2020).

Vertical wind shear also plays an important role in TC intensity changes, with its important role in TC intensity changes near the U.S. coast being noted by Kossin (2017). The VWS ahead of both Ida and Katrina was weak (ranging from 0 to 6 m s^{-1}) (Figs. 5a,b), favoring intensification of both systems (Fig. 5b). However, when both storms approached the coastline, the overland VWS in Ida became weaker (0–6 m s^{-1}) than for Katrina (6–15 m s^{-1}) (Figs. 5c,d). Ida's nearshore intensification and slow decay after landfall may be partially explained by generally weak VWS near the coast prior to landfall and then over land following landfall. The relatively strong over land VWS was unfavorable for Katrina, aiding in its more rapid decay.
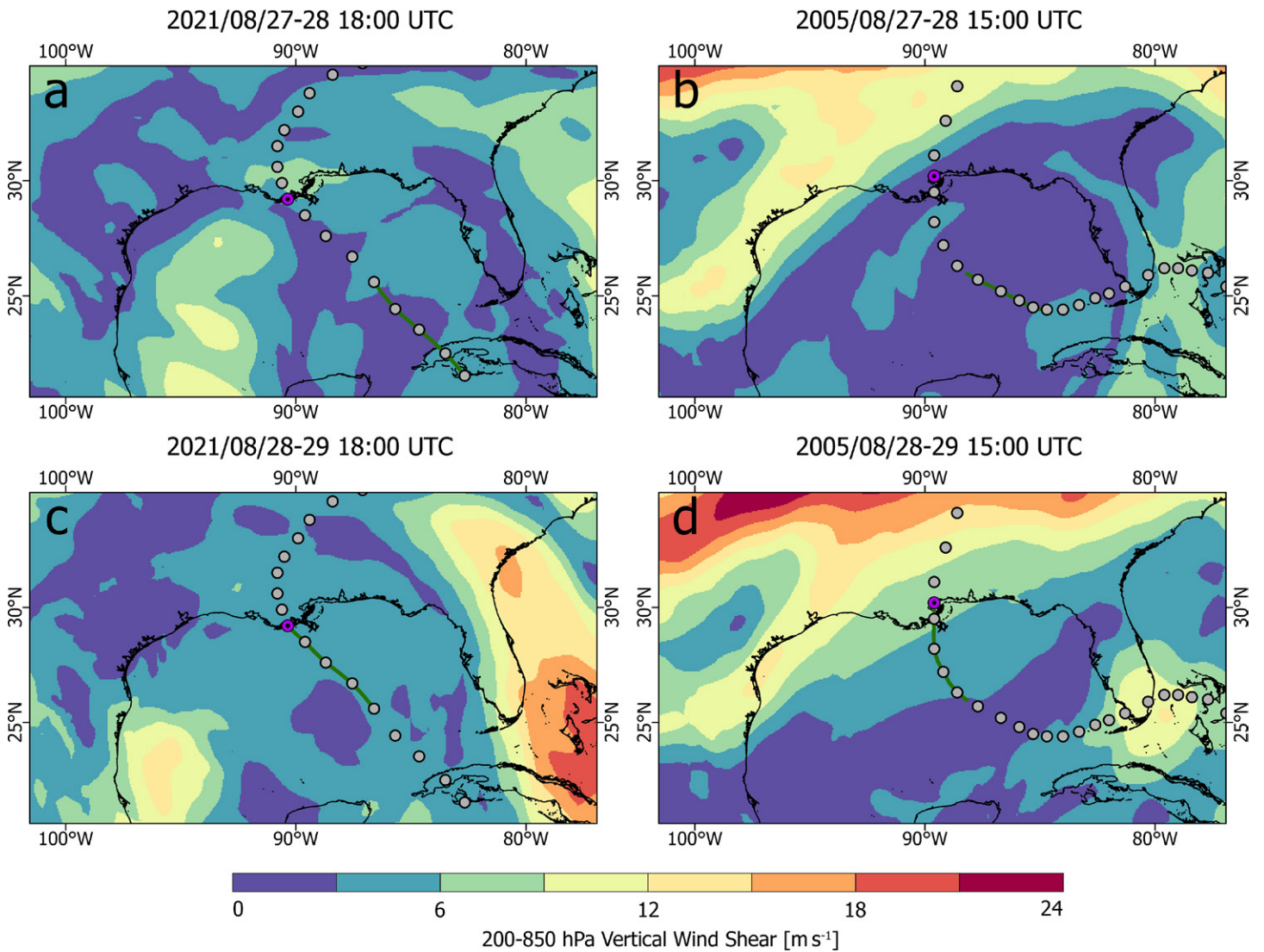
Fig. 5. As in Fig. 3, but for 200–850 hPa vertical wind shear.

Aside from intensity changes, we also note that the translation speed of the two hurricanes was quite different. Katrina moved relatively slow over the ocean with an average translation speed of ~22 km h^{-1} in the day before landfall and accelerated to an average of ~29 km h^{-1} in the first 24 h after landfall. By comparison, Ida also approached the coast with a 24-h-average forward speed of ~22 km h^{-1} in the day before landfall but decelerated with an average forward speed of ~15 km h^{-1} in the day following landfall. Ida's slower movement following landfall was particularly favorable for its weaker intensity decay, since a portion of the TC circulation remained over water (DeMaria et al. 2006). The storm motion differences can largely be explained by the intensity of the deep-layer meridional steering wind. For Ida, northward flow during the 48–24 h prelandfall period was stronger than for Katrina (positive values indicate northward wind; Figs. 6a,b). However, when Katrina approached the coastline, the meridional steering flow that it encountered strengthened considerably (Fig. 6d). By contrast, the northward steering flow ahead of Ida remained stable and relatively weak as the storm was making landfall (Fig. 6c).

In addition to atmospheric conditions, the impact of the land surface on TC inland decay, with a special focus on soil wetness, has been widely discussed (e.g., Kishtawal et al. 2012; Zhang et al. 2019). The soil moisture prior to Ida's landfall (Figs. 7a,c), as measured by the top layer of the volumetric soil water, was relatively greater than before Katrina's landfall (Figs. 7b,d). During the 48 h period before Ida's landfall, the mean volumetric soil water
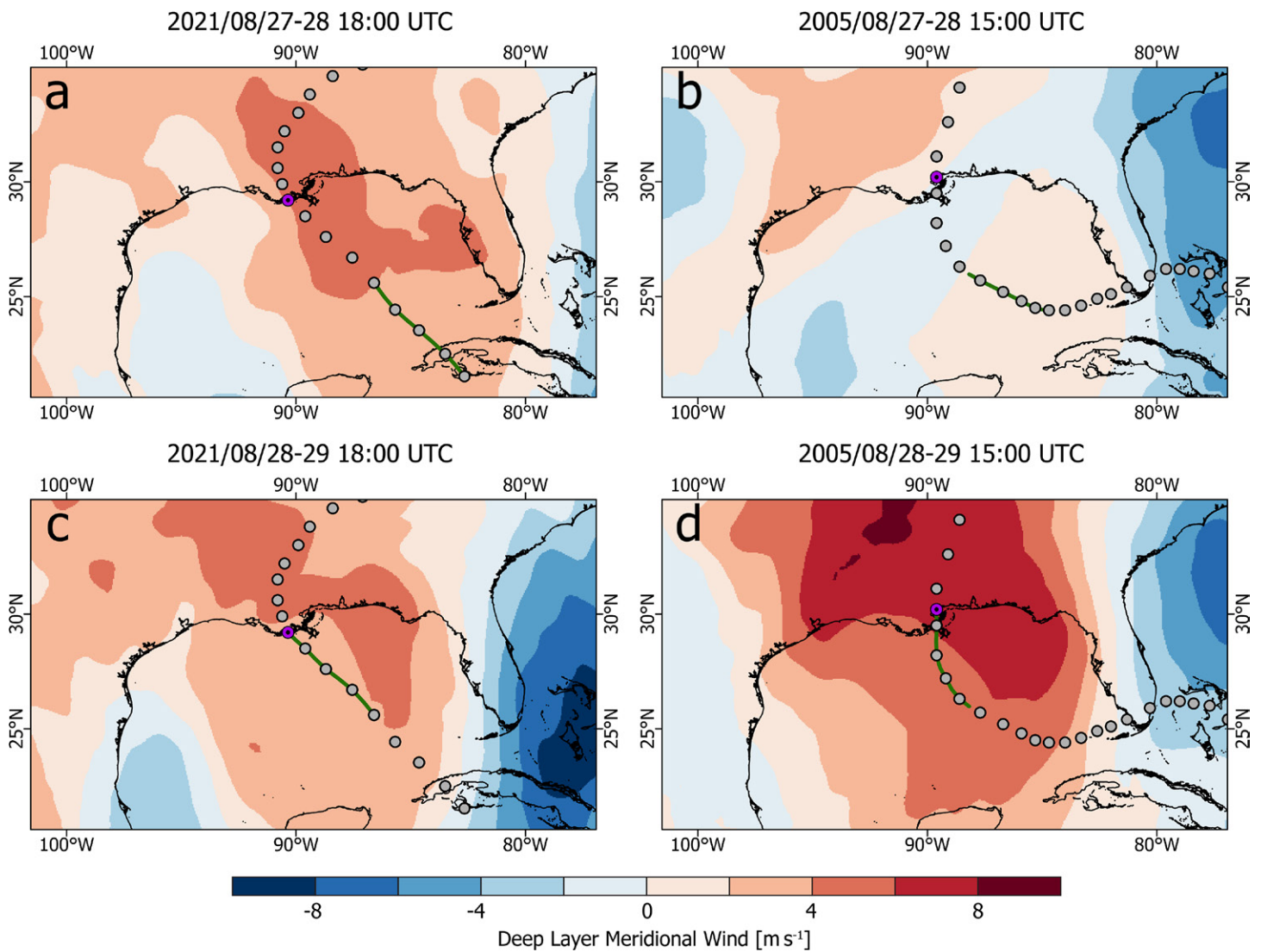
Fig. 6. As in Fig. 3, but for the deep-layer meridional steering flow.

within a 200 km radius of landfall location was 0.37 m³ m⁻³, which was more abundant than Katrina's 0.30 m³ m⁻³. This result was also implied by the observed midlevel RH, as discussed earlier (Fig. 4a). Increased antecedent soil moisture can favor a TC to weaken at a slower rate following landfall (Andersen and Shepherd 2017). The small changes observed in top-level soil moisture during Ida's landfall will be further discussed in the "Nearshore conditions before and after landfall for Gulf major hurricanes (1983–2021)" section.

A modeling study of a tropical low that brought flooding rainfall to Louisiana in August 2016 showed that the low pressure area likely intensified due to a combination of wetlands that predominate across southern Louisiana combined with high levels of antecedent soil moisture (Nair et al. 2019). Figure 8 shows cumulative daily precipitation recorded in the 4 days prior to landfall from three airports located in the vicinity of where both Ida and Katrina made landfall (data obtained from the National Centers for Environmental Information at www.ncdc.noaa.gov/cdo-web/search). Southern Louisiana received considerable precipitation in the days before Ida's landfall, with especially high rainfall recorded at Baton Rouge. In the 3 days prior to the day that Katrina made landfall, <5 mm was recorded at any of the three stations, with Baton Rouge and Hattiesburg reporting no rainfall until the day that Katrina made landfall. The heavy rainfall leading up to Ida's landfall contributed to the soil moisture difference between the two cases.
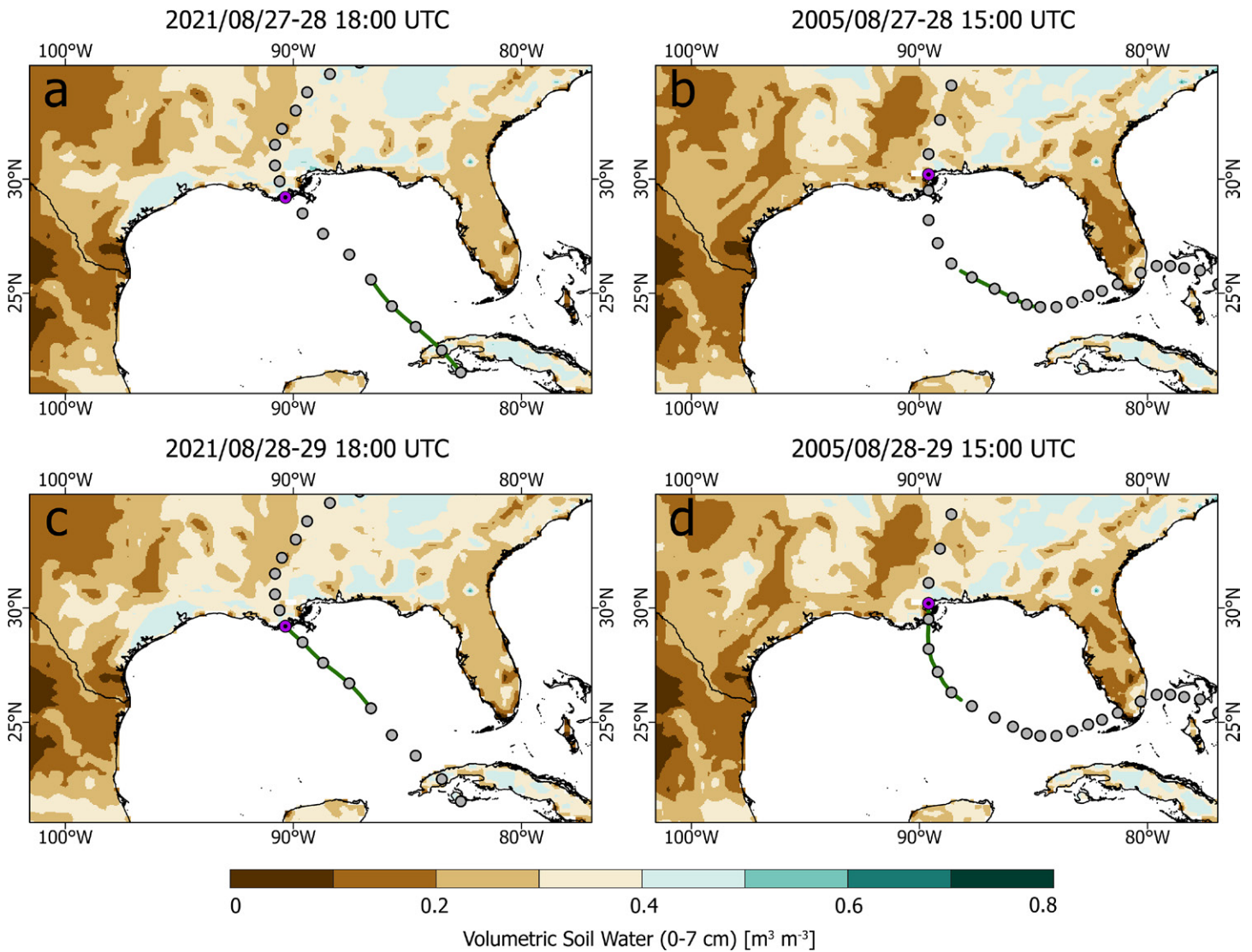
Fig. 7. As in Fig. 3, but for top-layer soil wetness.

Nearshore conditions before and after landfall for Gulf major hurricanes (1983–2021)
Pre- and postlandfall intensity changes for Hurricane Ida, Katrina, and other Gulf Coast major landfalling hurricanes are depicted in Fig. 9a. The widely used simple inland decay
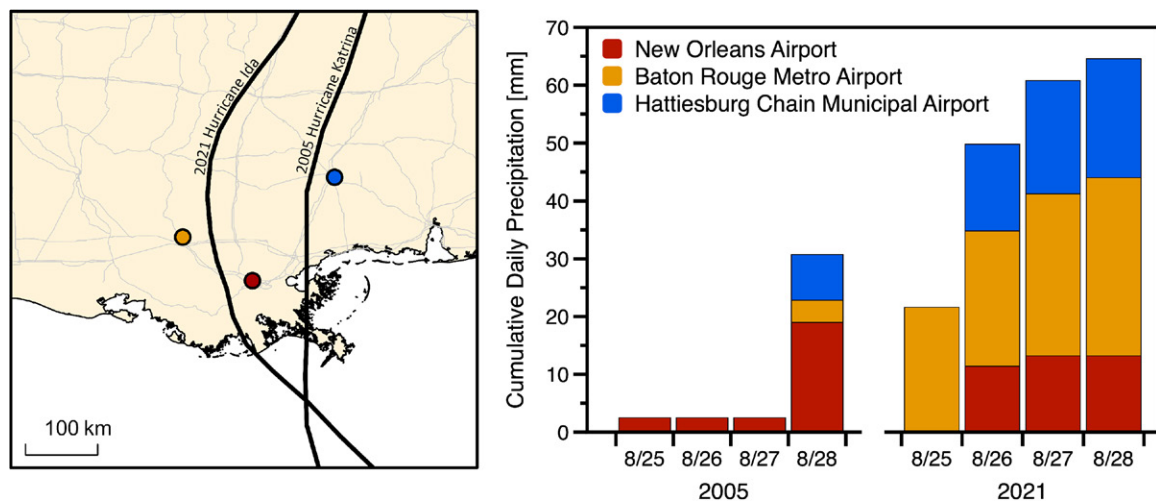

Fig. 8. Cumulative daily precipitation recorded at three airports near Katrina's and Ida's tracks.

model (Kaplan and DeMaria 1995, hereafter KD95) is employed to quantify postlandfall decay:

$$V(t) = V_b + (RV_o - V_b)e^{-at}. \quad (1)$$

Regional parameters for the Gulf Coast were used where $V_b = 25.5$ kt is the background wind speed, $R = 1$ is the reduction factor, V_o is the landfall MSW (kt), $a = 0.104$ is the decay constant (h^{-1}), and t refers to the time after landfall. The peak intensity of Katrina is among the highest of all landfalling cases, with Katrina also recording a rapid intensification of 50 kt in 24 h. However, the rapid intensification was followed by a quick decay in the next 24 h, with Katrina rapidly dissipating after landfall. The rapid decay of Katrina is well captured by the KD95 model, as is the reference set of major landfalling hurricane events. By comparison, Hurricane Ida gradually intensified during 48–24 h prior to landfall but then rapidly intensified within 24 h before landfall. Ida's intensification rate peaked at 55 kt (24 h)$^{-1}$ in the 30–6 h period prior to landfall. In addition to its rapid nearshore intensification, Ida's first 12 h postlandfall intensity decrease was significantly less than other major landfalling hurricane cases.

The nearshore SST generally decreases when storms pass over, causing a cold wake (Chen et al. 2017; Cione and Uhlhorn 2003). Though the 500 km nearshore SST is similar between Ida and Katrina, they are well above the average and significantly higher than other major Gulf Coast landfalling hurricanes (Fig. 9b). We note that the reference set only consists of major landfalling hurricanes. For these storms, the average SST on the day prior to landfall
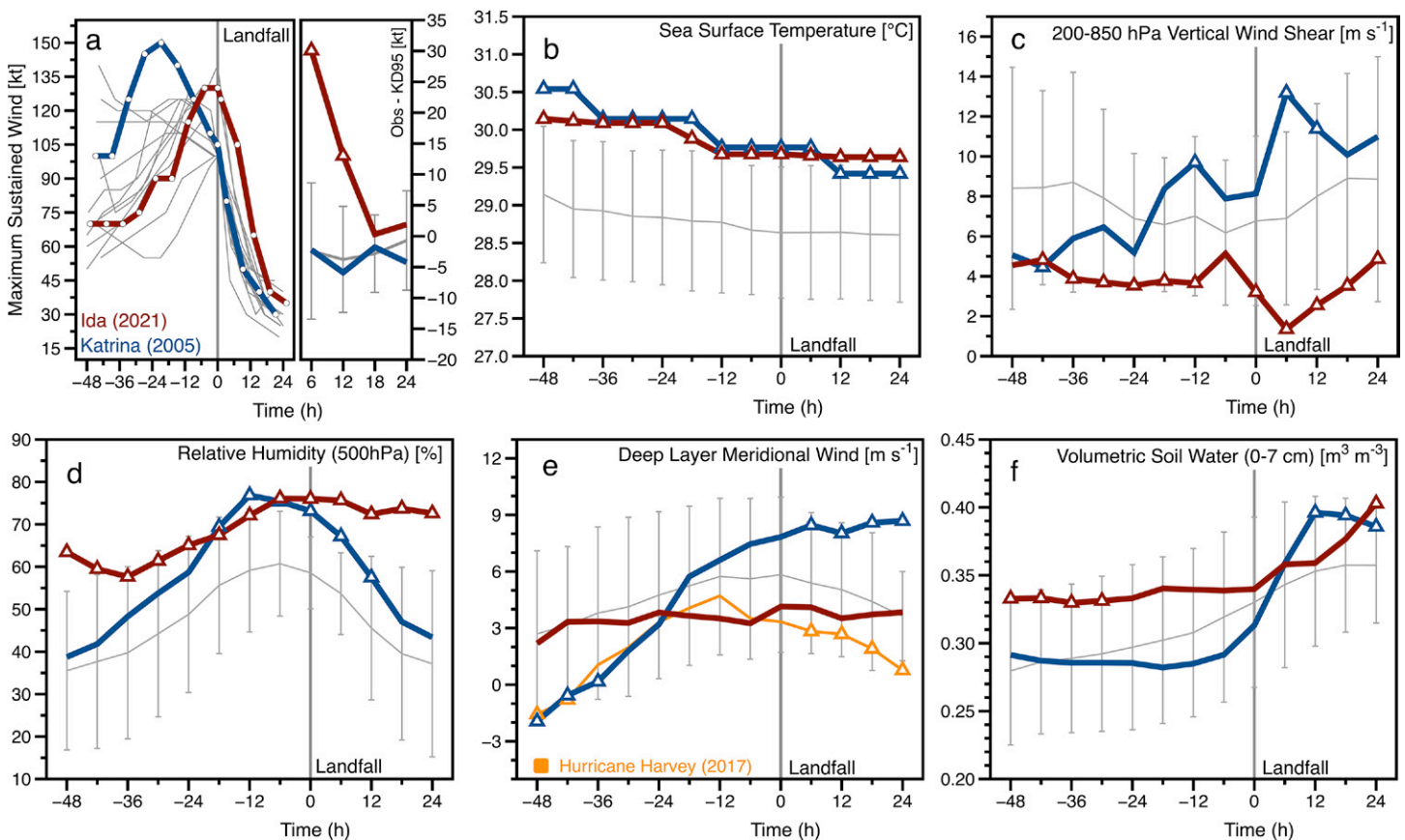

Fig. 9. (a) Intensity changes of Gulf of Mexico major hurricanes within 48 h prior to and 24 h after landfall, with the difference between the observed MSW and KD95 estimates during the postlandfall period. The gray line in the subpanel depicts the average from the reference major landfall events with one standard deviation indicated by the top and bottom of the bars. The reference set excludes Katrina. Triangles mark significance at the 5% level; (b) as in (a), but for changes in SST within the 500 km nearshore regions defined in Fig. 1. (c) As in (b), but for VWS; (d) as in (b), but for RH; (e) as in (b), but for meridional wind. Hurricane Harvey is displayed in yellow. (f) As in (b), but for top-layer soil wetness.
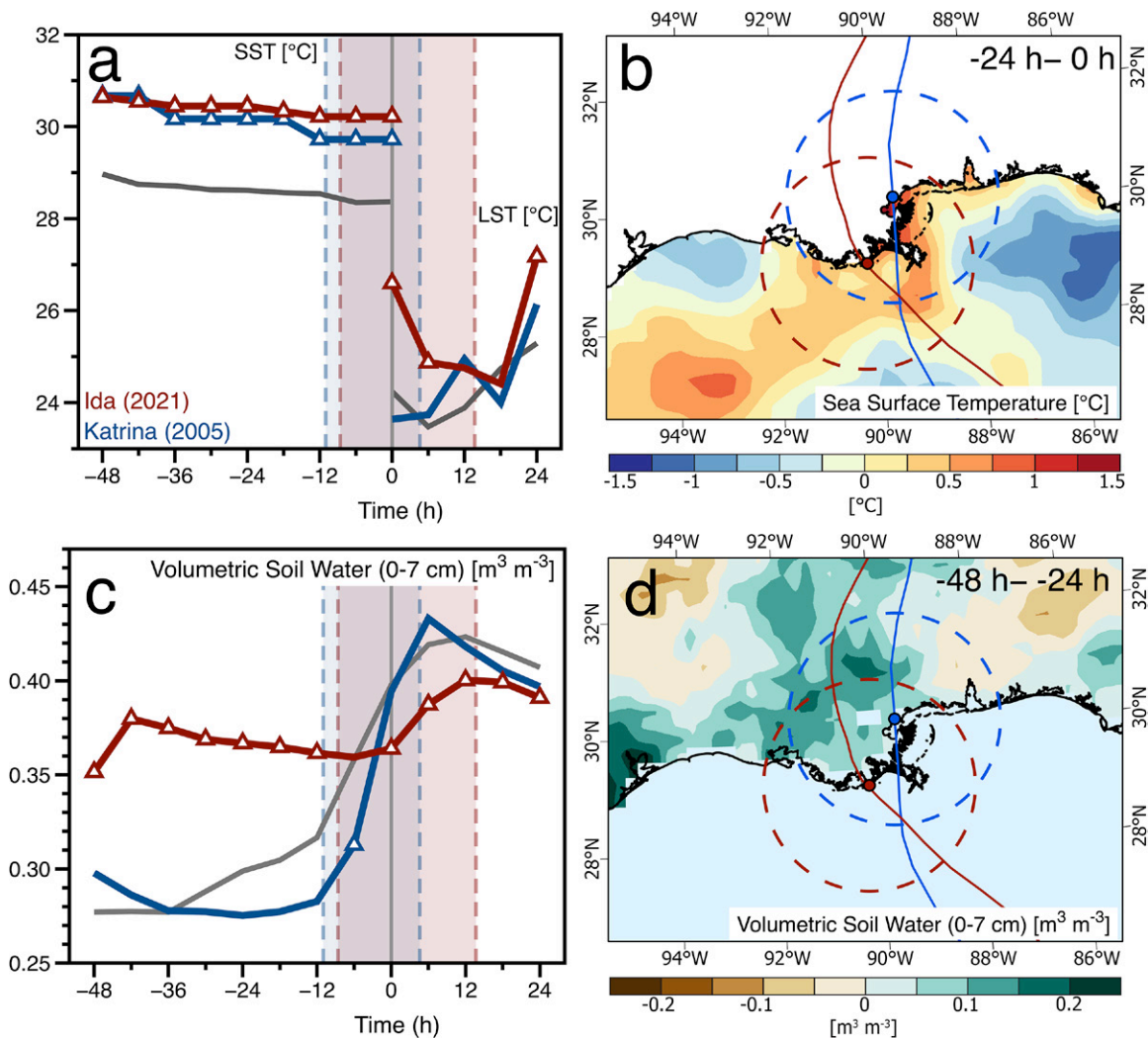
Fig. 10. (a) Changes in SST before landfall and land surface temperature (LST) after landfall within the 200 km nearshore regions defined in Fig. 1. The gray line indicates the average values from the reference major landfall events. Triangles mark significance at the 5% level. Areas bounded by the dashed lines mark the time when the storm center was inside the 200 km nearshore regions; **(b)** difference of the average SST during Ida and Katrina's final 24 h prior to landfall (e.g., Ida SST minus Katrina SST). The dashed circles depict the 200 km nearshore regions for both hurricanes; **(c)** as in (a), but for soil moisture; **(d)** as in (b), but for the average soil moisture 48–24 h before landfall.

was 28.7°C. However, nearshore SSTs for both Ida and Katrina were high anomalies from these other extreme events (e.g., other major landfalling Gulf Coast hurricanes). Since the intensification of hurricanes is more controlled by SST closer to the storm center, we also calculate SST closer to the storm center. The average 200 km nearshore SST during Ida's landfall is ~0.5°C higher than during Katrina's landfall (Fig. 10a), particularly near the coast (Fig. 10b).

By comparison, the averaged VWS within the nearshore region distinguishes Ida from Katrina, with Ida's value significantly lower than the average major landfalling Gulf hurricane when the storm approached and crossed the coastline (Fig. 9c). Increasing VWS as Katrina approached the coastline inhibited further intensification, agreeing with the findings from McTaggart-Cowan et al. (2007). Since strong VWS inhibits nearshore intensification and also favors inland decay, it could potentially explain the observed relationship between nearshore intensification and landfall dissipation as documented by Zhu et al. (2021).

The average nearshore midlevel RH follows a pattern that would be expected; that is, RH increases when storms approach the coastline and decreases after the storm moves inland or dissipates (Fig. 9d). During Katrina's landfall, the average nearshore RH showed a similar

pattern as the reference set but was relatively higher. Likewise, the average nearshore RH for Ida was significantly above the reference set at all time periods. The high RH value during 48–24 h prior to Ida's landfall reflects the heavy rainfall that occurred over southern Louisiana. The anomalously high RH from both storms could be partly explained by their passage over very warm SSTs, as storms passing over a warm ocean are supplied with high levels of moisture (Li and Chakraborty 2020). However, the RH does not decrease quickly following Ida's landfall, unlike what occurred in Katrina and most other Gulf Coast landfalling major hurricanes. Ida's RH values remain significantly higher than other Gulf Coast landfalling major hurricanes for the first 24 h after landfall. This is likely due to the slower movement of Ida once it made landfall. Though the high RH from Ida and Katrina was theoretically favorable for potential nearshore intensification (Kaplan and DeMaria 2003; Hendricks et al. 2010), higher VWS during Katrina's landfall was likely the primary reason why the storm weakened.

The average meridional wind generally increases when the storms enter the nearshore region (~24 h before landfall; Fig. 9e). As the meridional wind partially controls the translation speed of landfalling hurricanes in the Gulf of Mexico (Hassanzadeh et al. 2020), a decrease in the northward steering flow favors a slowdown in storm movement and potentially magnifies risks (i.e., rainfall) in coastal regions (Hall and Kossin 2019). The weak nearshore-average meridional steering flow (~3.5 m s^{-1}) during Ida's landfall helps explain the slow translation speed as the storm made landfall, whereas the significantly higher meridional steering flow during Katrina's landfall favors the storm's acceleration away from the coast. A significant weakening of the meridional steering flow occurred with 2017 Hurricane Harvey when the storm slowed to a crawl following landfall in Texas (translation speed of 5.7 km h^{-1} during the first 24 h after landfall). In contrast, the increasing northward steering flow during Katrina's landfall caused the storm to accelerate away from the warm ocean, favoring Katrina's rapid decay after landfall (Fig. 9e).

The nearshore soil moisture, similar to the midlevel RH, gradually increases when storms approach the coastline (Fig. 9f), due to heavy precipitation falling along the coast. However, the soil wetness level was already high 48 h prior to Ida's landfall due to copious precipitation in southern Louisiana from 26 to 28 August 2021. This antecedent high soil wetness prior to Ida's landfall is more obvious within the 200 km radius that represents the most active region for surface–air interaction (Fig. 10c), especially in southern Louisiana (Fig. 10d). For Katrina, the average soil wetness surged right after the storm entered the 200 km radius, showing a similar pattern to the reference set, with the increase of soil moisture mostly brought by the precipitation from the storm. The increase of soil moisture by along-track precipitation has been argued to contribute only minimally to the intensification of landfalling hurricanes (Evans et al. 2011; Zhang et al. 2019). These findings help explain why higher soil water content during Katrina's landfall did not lead to slower postlandfall intensity decay. We do note that in addition to soil wetness, the reduction of surface ground temperature under the center of the storm also favors the rapid intensity decay of a landfalling hurricane (e.g., Shen et al. 2002; Hlywiak and Nolan 2021). In an idealized framework, land surface temperature drops when the storm makes landfall but generally increases after landfall (Tuleya 1994). Within the 200 km radius of Ida's landfall, the significantly high nearshore SST and land surface temperature (LST) (26.6°C) at landfall provided favorable conditions for weak inland decay (Fig. 10a). Recent studies have also shown that land roughness significantly impacts postlandfall intensity decay, particularly for strong hurricanes (Chen and Chavas 2020; Hlywiak and Nolan 2021). Since the topography of Ida and Katrina's landfall locations are nearly identical, this effect is likely minimal in explaining the different decay processes between the two storms. However, the similar land surface characteristics of Ida and Katrina could be good cases for future studies isolating land roughness in simulation studies related to inland intensity decay.

In addition to the environmental factors discussed in this manuscript, hurricane nearshore intensity changes are also governed by internal dynamics. During Katrina's landfall, an eyewall replacement cycle was detected. Eyewall replacement processes generally cause storm weakening during the degeneration of the inner eyewall but reintensification after the complete formation of the new eyewall (Willoughby et al. 1982; Wang 2012). This process usually takes 1–2 days to complete (Sitkowski et al. 2011). However, Katrina's eyewall replacement occurred relatively close to landfall, where the formation of the new outer eyewall was not yet complete when the inner eyewall degenerated (Knabb et al. 2005). An eyewall replacement cycle was beginning when Ida was making landfall, but the process was just starting when the storm reached the coastline. Consequently, eyewall replacement cycle dynamics likely had relatively little impact on Ida's landfall intensity.

Conclusions

In this manuscript, we investigated environmental factors in the 48 h prior to extending up to the 24 h following the landfall of Hurricane Ida, Hurricane Katrina, and other Gulf landfalling major hurricanes since 1983. Though both Ida and Katrina shared very similar characteristics in terms of their landfall location and date, their nearshore and postlandfall intensity evolution were quite different. We first compared the environmental factors during the final 48 h before Ida's and Katrina's landfall. The nearshore conditions for these two storms were then compared to other historical major landfalling hurricanes over the Gulf Coast. Sea surface temperatures were quite favorable for both Ida and Katrina near the time of their landfall, although Ida's SSTs were particularly favorable for nearshore intensification. The nearshore SSTs during these two landfalling events were well above the average value from other Gulf Coast major landfalling hurricane events, but LSTs at the time of Ida's landfall were significantly higher. Similarly, midlevel RH conditions were favorable for both storms to retain their intensity or undergo intensification, but nearshore RH was higher ahead of Ida than it was ahead of Katrina. Ida and Katrina also brought a higher-than-average amount of midlevel moisture to the nearshore environment, given the greater storm moisture caused by higher SST (Li and Chakraborty 2020).

Unlike Katrina and the average of other major landfalling hurricane events, nearshore RH values changed very little during Ida's first 24 h following landfall. This result could be explained by Ida's slow inland movement following landfall. The slow translation speed of Ida following landfall can be attributed to weak northward steering flow. By contrast, southerly meridional winds strengthened and remained elevated during Katrina's landfall, supporting the acceleration of Katrina northward as it approached the coast and then moved onshore. Significantly stronger VWS during Katrina's landfall also inhibited the storm from retaining its intensity, while weak VWS along Ida's landfall trajectory favored the storm retaining its intensity. Copious precipitation in southern Louisiana and Mississippi in late August 2021 contributed to high soil moisture levels ahead of Ida's landfall. The soil water content was relatively low before Katrina's landfall in 2005. Higher soil moisture content potentially supports weaker intensity decay of postlandfalling hurricanes.

While this study compares the role that different nearshore environmental factors played in Ida, Katrina, and other major landfalling hurricanes over the Gulf Coast, further research is warranted on other factors such as the storm's internal dynamics, as well as quantification of each environmental factor through model simulations. While strong VWS inhibits the intensification of hurricanes, this protective barrier that is often near the northern Gulf Coast could weaken in a warming climate. Ting et al. (2019) found that, while overall VWS over the Gulf of Mexico is projected to be stronger by the end of the twenty-first century when compared to the end of the twentieth century, nearshore and inland VWS were weaker. This could favor more frequent nearshore intensification and weaker postlandfall intensity decay.

Data availability statement. All original data used in this study are publicly available. The TC data were obtained from the International Best Track Archive for Climate Stewardship version 4: www.ncdc. noaa.gov/ibtracs/. Tropical cyclone landfall data are from the Atlantic Oceanographic and Meteorological Laboratory: www.aoml.noaa.gov/hrd/hurdat/UShurrs_detailed.html. ERA5 data were downloaded from https://cds.climate.copernicus.eu/#!/search?text=ERA5&type=dataset. Precipitation data are obtained from the National Centers for Environmental Information at www.ncdc.noaa.gov/cdo-web/search.

References

Andersen, T., and M. Shepherd, 2017: Inland tropical cyclones and the "brown ocean" concept. *Hurricanes and Climate Change*, J. M. Collins and K. Walsh, Eds., Springer, 117–134, https://doi.org/10.1007/978-3-319-47594-3_5.

Beven, J. L., II, A. Hagen, and R. Berg, 2022: Tropical cyclone report: Hurricane Ida. National Hurricane Center Rep., 163 pp., www.nhc.noaa.gov/data/tcr/AL092021_Ida.pdf.

Chen, J., and D. R. Chavas, 2020: The transient responses of an axisymmetric tropical cyclone to instantaneous surface roughening and drying. *J. Atmos. Sci.*, **77**, 2807–2834, https://doi.org/10.1175/JAS-D-19-0320.1.

Chen, S., R. L. Elsberry, and P. A. Harr, 2017: Modeling interaction of a tropical cyclone with its cold wake. *J. Atmos. Sci.*, **74**, 3981–4001, https://doi.org/10.1175/JAS-D-16-0246.1.

Cione, J. J., and E. W. Uhlhorn, 2003: Sea surface temperature variability in hurricanes: Implications with respect to intensity change. *Mon. Wea. Rev.*, **131**, 1783–1796, https://doi.org/10.1175//2562.1.

Delgado, S., C. W. Landsea, and H. Willoughby, 2018: Reanalysis of the 1954–63 Atlantic hurricane seasons. *J. Climate*, **31**, 4177–4192, https://doi.org/10.1175/JCLI-D-15-0537.1.

DeMaria, M., and J. Kaplan, 1994: Sea surface temperature and the maximum intensity of Atlantic tropical cyclones. *J. Climate*, **7**, 1324–1334, https://doi.org/10.1175/1520-0442(1994)007<1324:SSTATM>2.0.CO;2.

——, J. A. Knaff, and J. Kaplan, 2006: On the decay of tropical cyclone winds crossing narrow landmasses. *J. Appl. Meteor. Climatol.*, **45**, 491–499, https://doi.org/10.1175/JAM2351.1.

Emanuel, K., 2007: Environmental factors affecting tropical cyclone power dissipation. *J. Climate*, **20**, 5497–5509, https://doi.org/10.1175/2007JCLI1571.1.

Evans, C., R. S. Schumacher, and T. J. Galarneau Jr., 2011: Sensitivity in the overland reintensification of Tropical Cyclone Erin (2007) to near-surface soil moisture characteristics. *Mon. Wea. Rev.*, **139**, 3848–3870, https://doi.org/10.1175/2011MWR3593.1.

Galarneau, T. J., and C. A. Davis, 2013: Diagnosing forecast errors in tropical cyclone motion. *Mon. Wea. Rev.*, **141**, 405–430, https://doi.org/10.1175/MWR-D-12-00071.1.

Gray, W. M., 1968: Global view of the origin of tropical disturbances and storms. *Mon. Wea. Rev.*, **96**, 669–700, https://doi.org/10.1175/1520-0493(1968)096<0669:GVOTOO>2.0.CO;2.

——, 1998: The formation of tropical cyclones. *Meteor. Atmos. Phys.*, **67**, 37–69, https://doi.org/10.1007/BF01277501.

Hall, T. M., and J. P. Kossin, 2019: Hurricane stalling along the North American coast and implications for rainfall. *npj Climate Atmos. Sci.*, **2**, 17, https://doi.org/10.1038/s41612-019-0074-8.

Hassanzadeh, P., C. Y. Lee, E. Nabizadeh, S. J. Camargo, D. Ma, and L. Y. Yeung, 2020: Effects of climate change on the movement of future landfalling Texas tropical cyclones. *Nat. Commun.*, **11**, 3319, https://doi.org/10.1038/s41467-020-17130-7.

Hendricks, E. A., M. S. Peng, B. Fu, and T. Li, 2010: Quantifying environmental control on tropical cyclone intensity change. *Mon. Wea. Rev.*, **138**, 3243–3271, https://doi.org/10.1175/2010MWR3185.1.

Hersbach, H., and Coauthors, 2020: The ERA5 global reanalysis. *Quart. J. Roy. Meteor. Soc.*, **146**, 1999–2049, https://doi.org/10.1002/qj.3803.

Hlywiak, J., and D. S. Nolan, 2021: The response of the near-surface tropical cyclone wind field to inland surface roughness length and soil moisture content during and after landfall. *J. Atmos. Sci.*, **78**, 983–1000, https://doi.org/10.1175/JAS-D-20-0211.1.

Kaplan, J., and M. DeMaria, 1995: A simple empirical model for predicting the decay of tropical cyclone winds after landfall. *J. Appl. Meteor.*, **34**, 2499–2512, https://doi.org/10.1175/1520-0450(1995)034<2499:ASEMFP>2.0.CO;2.

——, and ——, 2003: Large-scale characteristics of rapidly intensifying tropical cyclones in the North Atlantic basin. *Wea. Forecasting*, **18**, 1093–1108, https://doi.org/10.1175/1520-0434(2003)018<1093:LCORIT>2.0.CO;2.

Kellner, O., D. Niyogi, M. Lei, and A. Kumar, 2012: The role of anomalous soil moisture on the inland reintensification of Tropical Storm Erin 2007. *Nat. Hazards*, **63**, 1573–1600, https://doi.org/10.1007/s11069-011-9966-6.

Kishtawal, C. M., D. Niyogi, A. Kumar, M. L. Bozeman, and O. Kellner, 2012: Sensitivity of inland decay of North Atlantic tropical cyclones to soil parameters. *Nat. Hazards*, **63**, 1527–1542, https://doi.org/10.1007/s11069-011-0015-2.

Knabb, R. D., J. R. Rhome, and D. P. Brown, 2005: Tropical cyclone report: Hurricane Katrina. National Hurricane Center Rep., 43 pp., www.nhc.noaa.gov/data/tcr/AL122005_Katrina.pdf.

Knapp, K. R., M. C. Kruk, D. H. Levinson, H. J. Diamond, and C. J. Neumann, 2010: The International Best Track Archive for Climate Stewardship (IBTrACS): Unifying tropical cyclone data. *Bull. Amer. Meteor. Soc.*, **91**, 363–376, https://doi.org/10.1175/2009BAMS2755.1.

Kossin, J. P., 2017: Hurricane intensification along United States coast suppressed during active hurricane periods. *Nature*, **541**, 390–393, https://doi.org/10.1038/nature20783.

Landsea, C. W., 2007: Counting Atlantic tropical cyclones back to 1900. *Eos, Trans. Amer. Geophys. Union*, **88**, 197–202, https://doi.org/10.1029/2007EO180001.

——, and J. L. Franklin, 2013: Atlantic hurricane database uncertainty and presentation of a new database format. *Mon. Wea. Rev.*, **141**, 3576–3592, https://doi.org/10.1175/MWR-D-12-00254.1.

Li, L., and P. Chakraborty, 2020: Slower decay of landfalling hurricanes in a warming world. *Nature*, **587**, 230–234, https://doi.org/10.1038/s41586-020-2867-7.

Lok, C. C., J. C. Chan, and R. Toumi, 2021: Tropical cyclones near landfall can induce their own intensification through feedbacks on radiative forcing. *Commun. Earth Environ.*, **2**, 184, https://doi.org/10.1038/s43247-021-00259-8.

McTaggart-Cowan, R., L. F. Bosart, J. R. Gyakum, and E. H. Atallah, 2007: Hurricane Katrina (2005). Part I: Complex life cycle of an intense tropical cyclone. *Mon. Wea. Rev.*, **135**, 3905–3926, https://doi.org/10.1175/2007MWR1875.1.

——, E. L. Davies, J. G. Fairman, T. J. Galarneau, and D. M. Schultz, 2015: Revisiting the 26.5°C sea surface temperature threshold for tropical cyclone development. *Bull. Amer. Meteor. Soc.*, **96**, 1929–1943, https://doi.org/10.1175/BAMS-D-13-00254.1.

Nair, U. S., and Coauthors, 2019: Influence of land cover and soil moisture based brown ocean effect on an extreme rainfall event from a Louisiana Gulf Coast tropical system. *Sci. Rep.*, **9**, 17136, https://doi.org/10.1038/s41598-019-53031-6.

NOAA, 2022: Costliest U.S. tropical cyclones. NOAA Doc., 5 pp., www.ncdc.noaa.gov/billions/dcmi.pdf.

Saunders, M. A., P. J. Klotzbach, and A. S. Lea, 2017: Replicating annual North Atlantic hurricane activity 1878–2012 from environmental variables. *J. Geophys. Res. Atmos.*, **122**, 6284–6297, https://doi.org/10.1002/2017JD026492.

Schott, T., and Coauthors, 2012: The Saffir–Simpson hurricane wind scale. National Hurricane Center Doc., 4 pp., www.nhc.noaa.gov/pdf/sshws.pdf.

Shen, W., I. S. Ginis, and R. E. Tuleya, 2002: A numerical investigation of land surface water on landfalling hurricanes. *J. Atmos. Sci.*, **59**, 789–802, https://doi.org/10.1175/1520-0469(2002)059<0789:ANIOLS>2.0.CO;2.

Sitkowski, M., J. P. Kossin, and C. M. Rozoff, 2011: Intensity and structure changes during hurricane eyewall replacement cycles. *Mon. Wea. Rev.*, **139**, 3829–3847, https://doi.org/10.1175/MWR-D-11-00034.1.

Ting, M., J. P. Kossin, S. J. Camargo, and C. Li, 2019: Past and future hurricane intensity change along the US east coast. *Sci. Rep.*, **9**, 7795, https://doi.org/10.1038/s41598-019-44252-w.

Tuleya, R. E., 1994: Tropical storm development and decay: Sensitivity to surface boundary conditions. *Mon. Wea. Rev.*, **122**, 291–304, https://doi.org/10.1175/1520-0493(1994)122<0291:TSDADS>2.0.CO;2.

Wang, Y., 2012: Recent research progress on tropical cyclone structure and intensity. *Trop. Cyclone Res. Rev.*, **1**, 254–275, https://doi.org/10.6057/2012TCRR02.05.

Willoughby, H. E., J. A. Clos, and M. G. Shoreibah, 1982: Concentric eye walls, secondary wind maxima, and the evolution of the hurricane vortex. *J. Atmos. Sci.*, **39**, 395–411, https://doi.org/10.1175/1520-0469(1982)039<0395: CEWSWM>2.0.CO;2.

Wu, L., and Coauthors, 2012: Relationship of environmental relative humidity with North Atlantic tropical cyclone intensity and intensification rate. *Geophys. Res. Lett.*, **39**, L20809, https://doi.org/10.1029/2012GL053546.

Zhang, F., Z. Pu, and C. Wang, 2019: Impacts of soil moisture on the numerical simulation of a post-landfall storm. *J. Meteor. Res.*, **33**, 206–218, https://doi.org/10.1007/s13351-019-8002-8.

Zhu, Y. J., J. M. Collins, and P. J. Klotzbach, 2021: Nearshore hurricane intensity change and post-landfall dissipation along the United States Gulf and East Coasts. *Geophys. Res. Lett.*, **48**, e2021GL094680, https://doi.org/10.1029/2021GL094680.